

many valuable discussions.

\*Work supported by the U. S. Atomic Energy Commission under Contract No. AT(11-1)2126. It has also benefited from the general support of Materials Science at the University of Chicago provided by the Advanced Research Projects Agency.

†Deutsche Forschungsgemeinschaft Fellow.

‡Research supported in part by the National Science Foundation.

<sup>1</sup>J. S. Kasper and S. M. Richards, *Acta Crystallogr.* **17**, 752 (1964).

<sup>2</sup>D. E. Polk, *J. Non-Cryst. Solids* **5**, 365 (1971).

<sup>3</sup>F. P. Bundy and J. S. Jasper, *Science* **139**, 340 (1963).

<sup>4</sup>R. H. Wentorf, Jr., and J. S. Kasper, *Science* **139**, 338 (1963).

<sup>5</sup>J. H. Parker, Jr., D. W. Feldman, and M. Askin, *Phys. Rev.* **155**, 712 (1967).

<sup>6</sup>R. Alben, M. Thorpe, D. Weaire, and S. Goldstein,

to be published.

<sup>7</sup>To our knowledge, no optical measurements of the absorption edge of Si III or Ge III have been reported to date. However, as a crude approximation we assume that, at 5145 Å, the absorption coefficients of Ge III and Si III are of the same order, respectively, as those for Ge I and Si I given, for example, by J. R. Sandercock, *Phys. Rev. Lett.* **28**, 237 (1972).

<sup>8</sup>S. A. Solin and A. K. Ramdas, *Phys. Rev. B* **1**, 1687 (1970).

<sup>9</sup>G. F. Koster, J. O. Dimmock, R. G. Wheeler, and H. Statz, *Properties of the 32 Point Groups* (Massachusetts Institute of Technology Press, Cambridge, Massachusetts, 1963).

<sup>10</sup>P. N. Keating, *Phys. Rev.* **145**, 637 (1966).

<sup>11</sup>F. Herman, *J. Phys. Chem. Solids* **8**, 405 (1959).

<sup>12</sup>G. Dolling, in *Inelastic Scattering of Neutrons in Solids and Liquids* (International Atomic Energy Agency, Vienna, 1963) Vol. 2, p. 37; also B. N. Brockhouse and P. K. Iyengar, *Phys. Rev.* **111**, 747 (1958).

## Induction Cyclotron Resonance\*

F. L. Galeener,† T. A. Evans,‡ and J. K. Furdyna

*Department of Physics, Purdue University, Lafayette, Indiana 47907*

(Received 24 May 1972)

An approximate theory is developed for the magnetic dipole response of a small semiconducting sphere placed in a cavity at a point of maximum microwave magnetic field. Experiments corroborate the prediction that electric fields induced in the particle lead to resonant absorption at an applied dc magnetic field free of depolarization (magnetoplasma) shifts. The effect may enable microwave determination of effective mass in materials having carrier concentrations well above the limit for conventional cyclotron resonance.

Conventional cyclotron resonance (CR) experiments at microwave frequencies<sup>1</sup> yield effective masses  $m^*$  only for materials having very low electron or hole concentrations,  $n$  (or  $p$ )  $< 10^{13}$   $\text{cm}^{-3}$ . At larger concentrations, the carriers in a bounded sample exhibit magnetoplasma resonance (MPR) which occurs at a magnetic field  $B$  essentially independent of  $m^*$ . To circumvent these bounded-sample effects and recover values of  $m^*$ , experimenters are forced to make measurements in the infrared, requiring extremely high magnetic fields.<sup>2</sup> MPR has been discussed by Dresselhaus, Kip, and Kittel<sup>1</sup> using the language of depolarization analysis, and has recently been related to electric dipole scattering by Galeener.<sup>3</sup> In this Letter, we extend the latter scattering treatment beyond the quasistatic regime and predict the existence of magnetic dipole response which peaks near the cyclotron resonance field and avoids the complications of MPR for carrier concentrations several orders of

magnitude greater than  $10^{13}$   $\text{cm}^{-3}$ . We call the phenomenon induction cyclotron resonance (ICR), and present microwave experiments<sup>4</sup> demonstrating its existence in  $n$ -type InSb samples having  $n$  up to  $4 \times 10^{14}$   $\text{cm}^{-3}$ .

Figure 1(a) depicts a  $\text{TE}_{102}$  microwave cavity of the type commonly used in resonance experiments. In conventional CR a small spherical sample is placed at a position of maximum cavity electric field  $\vec{E}_c$ , exemplified by point A in the figure. It is instructive first to discuss sample excitation in the absence of the applied magnetic field  $\vec{B}_{dc}$ . In that case  $\vec{E}_c$  unquestionably induces an electric dipole field in the interior of the sample similar to that shown in Fig. 1(b). The solenoidal  $\vec{H}$  field induced in the sample is usually ignored, and the response is treated in the quasistatic limit, where  $\vec{E}$  is uniform. The discontinuity of the normal component of electric displacement at the boundary requires the existence of a time-varying surface-charge layer, depicted schema-

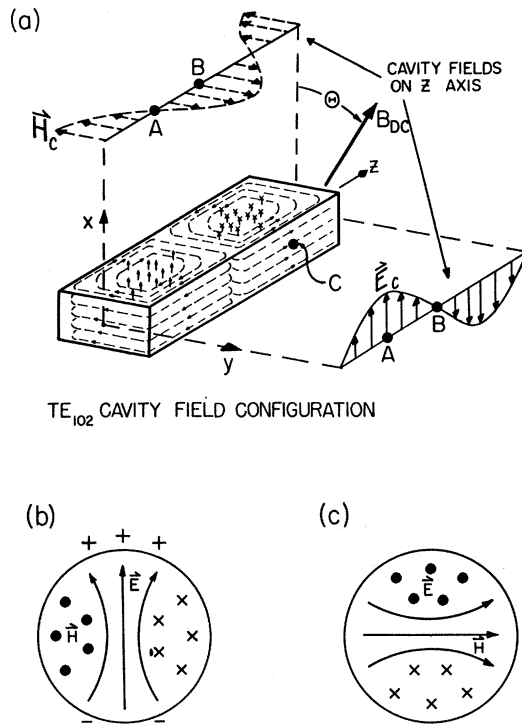


FIG. 1. (a) Cavity fields in a typical microwave resonance experiment. When  $B_{dc} = 0$  these excite (b) electric dipole fields in a dielectric sphere placed at point A and (c) magnetic dipole fields when placed at point B. Note that depolarization charges (+, -) are absent in (c), because  $\vec{E}$  is solenoidal (about  $\vec{H}$ ).

tically in Fig. 1(b). It is the presence of these "depolarization" charges, whose density increases with  $n$ , that gives rise to MPR and obscures the observation of CR.

Consider a sample placed in the cavity at point B in Fig. 1(a). We expect the driving  $\vec{H}$  field to excite a *magnetic* dipole field in the interior of the sample similar to that shown in Fig. 1(c). The fields are time varying so that the quasiuniform internal  $\vec{H}$  must in fact be accompanied by a solenoidal electric field  $\vec{E}$  which has negligible components normal to the sample surface. In this way, one should be able to probe the electrical conductivity of the sample without creating depolarization charge. We view the probing electric field as derived by *induction* from the driving microwave  $H$  field, hence our name for the phenomenon.

In the absence of an applied magnetic field, an InSb sample is isotropic and its contribution to cavity absorption can be measured by the extinction cross section  $\Sigma_{\text{ext}}$  for plane-wave scattering by a dielectric sphere, computed from the Mie

theory.<sup>5</sup> Under the assumption that internal and external fields vary little over the sphere diameter, we have evaluated the exact Mie theory in the so-called Rayleigh limit, finding that the electric ( $e$ ) and magnetic ( $m$ ) dipole cross sections are given by<sup>6,5,3</sup>

$$\Sigma_{\text{ext}}^e = 12\pi a^3 k_0 \kappa'' / [(\kappa' + 2)^2 + (\kappa'')^2], \quad (1)$$

$$\Sigma_{\text{ext}}^m = \frac{2}{15} \pi a^5 k_0^3 \kappa'', \quad (2)$$

where  $\kappa \equiv \kappa' + i\kappa''$  is the complex dielectric constant of the sample material and  $a$  is the radius of the sphere. Formally, the Rayleigh limit requires that  $|k_0 a| < 1$  and  $|ka| < 1$ , where  $k_0$  and  $k = k_0 \kappa^{1/2}$  are the complex propagation constants for plane waves in vacuum and bulk sample material, respectively.

When the applied magnetic field is nonzero ( $B \neq 0$ ), the electromagnetic scattering problem is greatly complicated because the sample has a *tensor* dielectric constant  $\kappa$  of the gyrotropic form<sup>7</sup>

$$\kappa = \begin{bmatrix} \kappa_{xx} & \kappa_{xy} & 0 \\ -\kappa_{xy} & \kappa_{xx} & 0 \\ 0 & 0 & \kappa_z \end{bmatrix}, \quad (3)$$

where  $\hat{z}$  is directed along the applied magnetic field  $\vec{B}$ . Calculation of electromagnetic scattering by such a gyroelectric sphere, of arbitrary size, has received considerable attention,<sup>8</sup> but remains an unsolved problem of classical electrodynamics.

In connection with earlier work<sup>9</sup> we have developed an *ad hoc* approximate solution<sup>6</sup> which successfully explains<sup>10</sup> major features of experiments on the dimensional resonances of magneto-plasma spheres reported by Cardona and Rosenblum.<sup>11</sup> It is well known that the gyroelectric tensor (3) is diagonalized in a coordinate system consisting of fields (normal to  $\hat{z}$ ) circularly polarized in the + and - senses about  $\hat{z}$ , and fields linearly polarized along  $\hat{z}$ , with corresponding principal dielectric constants denoted  $\kappa_+$ ,  $\kappa_-$ , and  $\kappa_z$ , respectively. At a given cavity position we decompose the electric and magnetic cavity fields (at sample center) into their +, -, and  $z$  components. We then calculate the sample absorption due to each driving field (+, -, or  $z$ ) as if the sample were an isotropic (Mie) sphere having the corresponding principal dielectric constant ( $\kappa_+$ ,  $\kappa_-$ , or  $\kappa_z$ , respectively).<sup>6</sup> In the Rayleigh limit this procedure is known to give exact results for the electric dipole case,<sup>3</sup> using Eq. (1).

Predictions for  $n$ -InSb are based on the fact that

this material can be described at microwave frequencies by a Drude dielectric tensor,<sup>12</sup> whose principal elements we write in the compact form

$$\kappa(B) = \kappa_l + ine\mu\omega^{-1}\epsilon_0^{-1}[1 - i\mu(B_{CR} + B)]^{-1}, \quad (4)$$

where  $\kappa_l$  is the lattice dielectric constant (19.6 for InSb),<sup>12</sup>  $\epsilon_0$  is the permittivity of free space,  $\omega$  the angular microwave frequency, and  $\mu$  the mobility of the electrons having concentration  $n$  and elementary charge  $e > 0$ . The true cyclotron resonance field is related to the effective mass by  $B_{CR} \equiv m^*\omega/e$ . Equation (4) suffices to determine all three principal dielectric constants according to the prescriptions  $\kappa(B < 0) = \kappa_+$ ;  $\kappa(B = 0) = \kappa_z$ ;  $\kappa(B > 0) = \kappa_-$ .

Combining these results we find that for *principal* excitations ( $E, H$ ) the absorbed power  $P$  is given approximately by

$$P^e = \frac{E^2}{Z_0} \sum_{\text{ext}} e = \frac{12\pi E^2 a^3 ne \mu (\kappa_l + 2)^{-2}}{1 + \mu^2 (B_{MPR} + B)^2}, \quad (5)$$

$$P^m = Z_0 H^2 \sum_{\text{ext}} m = \frac{\frac{2}{15} \pi Z_0^2 H^2 k_0^2 a^5 ne \mu}{1 + \mu^2 (B_{CR} + B)^2}, \quad (6)$$

where  $Z_0$  is the impedance for cavity waves ( $Z_0^2 \sim \mu_0/\epsilon_0$ , where  $\mu_0$  is the permeability of free space). Both of these expressions are perfect Lorentzians in the applied magnetic field having the same width at half-height,  $\Delta B = 2\mu^{-1}$ . The position of the electric dipole resonance (MPR) is given by

$$B_{MPR} = -B_{CR} + ne[\omega\epsilon_0(\kappa_l + 2)]^{-1},$$

while that of the magnetic dipole resonance (ICR) is given by

$$B_{ICR} = -B_{CR} = -m^*\omega/e.$$

Thus we predict that ICR will occur at the true cyclotron resonance field, independent of carrier concentration, and (within the Rayleigh limit) independent of particle size.

To test the above predictions we have carried out experiments on small  $n$ -InSb spheres using a 35-GHz double-conversion superheterodyne spectrometer equipped with a TE<sub>102</sub> rectangular cavity.<sup>4</sup> Typical recorder traces are shown in Fig. 2 for a sphere having  $a \approx 100 \mu\text{m}$  and placed near point  $B$  [in Fig. 1(a)]. A careful consideration of probable internal field configurations for  $\vec{B} \parallel \vec{H}$  and  $\vec{B} \perp \vec{H}$  (at point  $B$ ) suggests that the *magnetic* dipole excitations in the two cases may not be equivalent. Experimentally, a clear resonance is seen near 0.48 kG in Fig. 2(a) for  $\vec{B} \perp \vec{H}$ , while

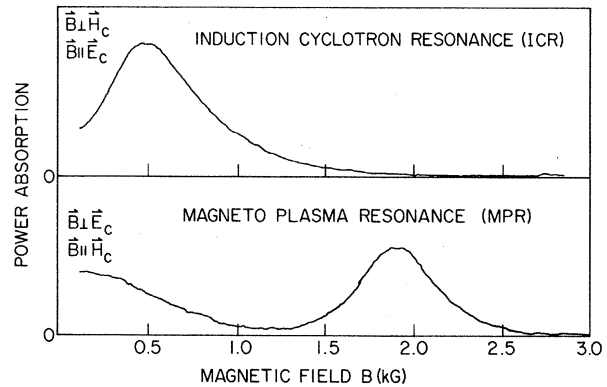


FIG. 2. Representative recorder traces for  $n$ -InSb sphere showing 0.48-kG ICR and 1.9-kG MPR observed near point  $B$  [in Fig. 1(a)].

a nonresonant absorption is found at lower fields in Fig. 2(b), where  $\vec{B} \parallel \vec{H}$ . The latter absorption appears to have some of the properties expected for ICR, but we were unable to resolve a peak. We have therefore concentrated our attention on the clearly resolvable peak labeled ICR in Fig. 2(a). The prominent peak seen at about 1.9 kG in Fig. 2(b) is MPR deliberately excited by placing the particle slightly off point  $B$ , where  $\vec{E} \neq 0$ . Detailed studies of the properties of these resonances will be reported elsewhere.<sup>13</sup> Their half-widths are approximately the same as predicted; MPR shows  $\Delta B \sim 0.5$  kG, indicating that  $\mu \sim 4 \times 10^5$  cm<sup>2</sup>/V sec. Elsewhere<sup>4,13</sup> we present experimental proof that the ICR peak indeed corresponds to  $B < 0$  [in Eqs. (4) and (8)] while the MPR peak corresponds to  $B > 0$ .

Other predictions of Eqs. (5) and (6) are verified by the experiments. For example, the strength of ICR at the peak varies accurately as the fifth power of particle size. Also, the strength of ICR varies accurately as the square of the *principal* component of  $\vec{H}_c$ ; in particular, it varies as  $\cos^2\theta$  when the field direction in Fig. 1(a) is rotated in steps from  $\vec{B}_{dc} \perp \vec{H}_c$  to  $\vec{B}_{dc} \parallel \vec{H}_c$ . MPR strength varies as  $\sin^2\theta$ . Spectra obtained at other points in the cavity, such as point  $C$  in Fig. 1(a), combine ICR and MPR response in about the proportions expected on the assumption that each is excited independently by the principal components of  $\vec{H}_c$  and  $\vec{E}_c$  obtaining at the center of the sphere. Experiments in the vicinity of 77°K indicate that linewidth varies with the inverse of the mobility, and line strength as the product of mobility and carrier concentration, as expected.

Figure 3 compares the predictions for resonance position, Eqs. (7) and (8), with experimen-

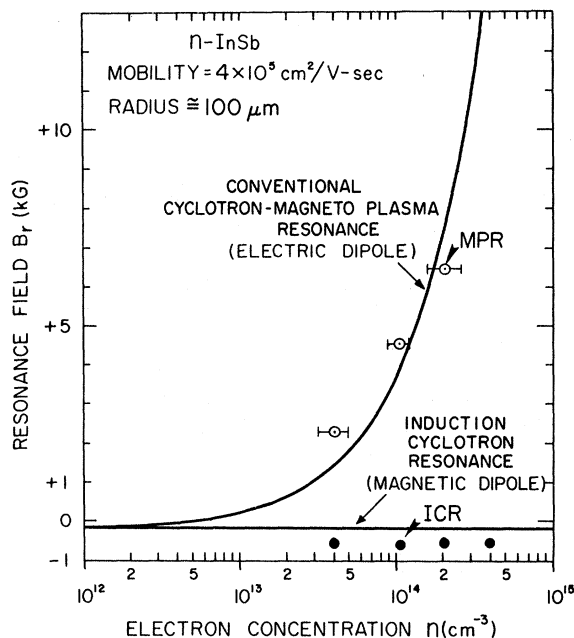


FIG. 3. Comparison of theoretical resonance fields with experimental results for MPR (open circles) and ICR (closed circles). ICR occurs at  $-0.48$  kG, free of the strong depolarization effects ( $n$  dependence) exhibited by MPR. Bars represent manufacturer's uncertainties in  $n$ .

tal observations at four carrier concentrations above the accessible range of conventional CR. Since pure  $n$ -InSb has  $m^* \approx 0.013m_e$ , the true cyclotron resonance field is  $-B_{CR} \approx -0.16$  kG. The upper curve [Eq. (7)] provides a satisfactory fit to the observed MPR points (open circles) and at the same time illustrates dramatically the extent of the deviation of MPR from the true cyclotron resonance field, marked by the lower horizontal curve. The solid points are the measured positions of ICR. Spheres with carrier concentrations in the range  $6 \times 10^{13}$  to  $4 \times 10^{14}$   $\text{cm}^{-3}$  and having radii from 50 to 135  $\mu\text{m}$  were measured and all exhibited ICR at the same field value,  $0.48 \pm 0.02$  kG. Thus our experimental observations show that within the Rayleigh limit the ICR field is indeed free of magnetoplasma effects (dependence on  $n$ ) and dimensional resonance effects (dependence on  $a$ ), as predicted.

The fact that we observe ICR in spheres at approximately 3 times the true CR value is the only apparent discrepancy between theory and experiment. If the discrepancy represents a failure of the theory, as we think likely, the phenomenon may still prove useful for effective-mass determination. Thus, experiments on materials with

differing known  $m^*$  might establish that the factor of essentially 3 is universal, dictated by the spherical geometry. (In this connection, it may be significant that the depolarization factor of a sphere is  $\frac{1}{3}$ , and that we experimentally observe shifted  $B_{ICR}$  in ellipsoidal samples.) We believe that further experimental effort and an attempt to construct a better mathematical solution in the Rayleigh limit are justified by the present results.

We remark that induction cyclotron resonance should have an analog in microwave cavity studies of magnetic materials. Demagnetization effects encountered there<sup>14</sup> ought to be diminished by placing the sample at a position of maximum cavity electric field.

One of us (F.L.G.) wishes to thank the Xerox Palo Alto Research Center for generous support during the period when final theoretical considerations and preparation of the manuscript were accomplished.

\*Work supported in part by the Advanced Research Projects Agency, the U. S. Army Research Office (Durham), the National Aeronautics and Space Administration, and the Purdue Research Foundation.

†Present address: Xerox Palo Alto Research Center, Palo Alto, California 94304.

‡Present address: General Electric Lighting Research Center and Technical Service Operation, Nela Park, Cleveland, Ohio 44112.

<sup>1</sup>G. Dresselhaus, A. F. Kip, and C. Kittel, *Phys. Rev.* **92**, 827 (1953), and **98**, 368 (1955), and **100**, 618 (1955).

<sup>2</sup>B. Lax and J. Mavroides, in *Solid State Physics*, edited by F. Seitz and D. Turnbull (Academic, New York, 1960), Vol. 11.

<sup>3</sup>F. L. Galeener, *Phys. Rev. Lett.* **22**, 1292 (1969).

<sup>4</sup>For discussion of experiment and theory see T. A. Evans, Ph. D. thesis, Purdue University, 1971 (University Microfilms, Ann Arbor, Michigan, 1971).

<sup>5</sup>See, e.g., H. C. van de Hulst, *Light Scattering by Small Particles* (Wiley, New York, 1957), Chap. 9. Also L. D. Landau and E. M. Lifshitz, *Electrodynamics of Continuous Media* (Pergamon, New York, 1960), p. 303 ff.

<sup>6</sup>For extensive discussion see F. L. Galeener, Ph. D. thesis, Purdue University, 1970 (University Microfilms, Ann Arbor, Michigan, 1970).

<sup>7</sup>B. Lax and L. M. Roth, *Phys. Rev.* **98**, 548 (1955).

<sup>8</sup>P. S. Epstein, *Rev. Mod. Phys.* **28**, 3 (1956); Y. J. Seto and A. A. Dougal, *J. Math. Phys.* **5**, 1326 (1964).

<sup>9</sup>F. L. Galeener and J. K. Furdyna, *Phys. Rev. B* **4**, 1853 (1971).

<sup>10</sup>F. L. Galeener, to be published. See also Ref. 6, Chap. 5.

<sup>11</sup>M. Cardona and B. Rosenblum, *Phys. Rev.* **128**, 1646

(1962).

<sup>12</sup>See, e.g., J. K. Furdyna, *Appl. Opt.* **6**, 675 (1967).<sup>13</sup>T. A. Evans and J. K. Furdyna, to be published.<sup>14</sup>B. Lax and K. J. Button, *Microwave Ferrites and Ferrimagnetics* (McGraw-Hill, New York, 1962), Chap. 4.

## Relationship between Atomic Structure and Electronic Properties of (111) Surfaces of Silicon\*

M. Erbudak and T. E. Fischer†

*Department of Engineering and Applied Science, Yale University, New Haven, Connecticut 06520*

(Received 26 June 1972)

The effect of annealing on electronic properties of vacuum-cleaved surfaces of Si is investigated by means of photoelectron and secondary-electron emission. It is found that annealing results in a change in the surface structure, which in turn influences the electronic properties of the surface, such as the work function, ionization energy, electron affinity, position of the Fermi level in the band gap, and spectrum of surface states.

Low-energy electron diffraction (LEED) studies<sup>1</sup> have shown that the arrangement of atoms on the (111) surface of Si represents three different structures that depend on the thermal history: The freshly cleaved surface has a  $2 \times 1$  superstructure; annealing at moderate temperatures produces a surface mesh of the same size as the projection of the bulk unit cell; and heating to  $800^\circ\text{C}$  results in a  $7 \times 7$  superstructure. The positions of the surface atoms in these structures are not yet known, but the existence of structural changes has been verified by numerous workers.

Measurement of electronic properties, and in particular of the spectrum of surface states, has been done mostly on the freshly cleaved (111) surface. Allen and Gobel<sup>2</sup> have first shown the existence of surface states by establishing the pinning of the Fermi level in the band gap at the surface. These measurements were later extended to lower temperatures.<sup>3</sup> Recently, Eden,<sup>4</sup> Eastman and Grobman,<sup>5</sup> and Wagner and Spicer<sup>6</sup> have obtained direct evidence from photoemission by excitation of electrons from the surface states of the freshly cleaved surface. Field emission from surface states on differently oriented surfaces has been reported by Lewis and Fischer.<sup>7</sup> Allen and Gobel<sup>8</sup> have shown that annealing changes the photoemission from the (111) surface of Si. No correlation between the electronic properties and the different structures of this surface has been investigated to date. This paper presents the results of a systematic study of such a correlation.

Clean surfaces were first exposed by cleavage *in situ*; their structure was later changed by several anneals at increasing temperatures. After each heat treatment, the samples were al-

lowed to cool and the structure was monitored by LEED and electronic properties were measured by photoelectron and secondary-emission spectroscopy at room temperature.

All measurements were performed in an ion-pumped stainless-steel vacuum system at pressures better than  $3 \times 10^{-11}$  Torr. A rotatable sample holder was equipped with a metallic emitter for Fermi-level determinations and experimental calibration.<sup>9</sup> Si crystals were cut in an L shape in cross section, exposing the (111) surfaces. This shape proved to give most satisfactory cleavages.<sup>10</sup> The results from four cleavages were exactly reproducible and agreed with those previously reported.<sup>2,3</sup>

We used 1- $\Omega$ -cm *n*-type crystals which were degassed by electron bombardment for more than 2 h at temperatures around  $1300^\circ\text{K}$ . This enabled us to maintain the very low pressures while annealing the samples ( $8 \times 10^{-11}$  Torr at  $1100^\circ\text{K}$ ). Evaporation of cathode material onto the surface was avoided by proper positioning of the filament.

Figure 1 shows the changes of the work function  $\phi$  as one anneals the cleaved crystal to successively higher temperatures. The dashed line in the same figure represents the position of the Fermi level in the band gap at the surface,  $(E_F - E_v)_s$ , for different annealing temperatures. It is in reasonable agreement with surface-conductivity measurements.<sup>11</sup> Both quantities plotted in Fig. 1 are obtained<sup>12</sup> from the shifts of the low- and high-energy ends of the energy distributions of photoelectrons shown in Fig. 2. The ionization potential  $\xi$  can be determined from the two quantities shown in Fig. 1 by the relation  $\xi = \phi + (E_F - E_v)_s$ .